Modeling and simulation of a reformate supplied PEM fuel cell stack, application to fault detection

Masoud Najafi, Damiano Dipenta, Karim Bencherif, Michel Sorine

Modeling and simulation of a reformate supplied PEM fuel cell stack, application to fault detection

M. Najafi,* D. Di Penta,† K. Bencherif,‡ and M. Sorine§

SOSSO2 Project, INRIA-Rocquencourt

Domaine de Voluceau, BP 105

78153, Le Chesnay, France¶

A method to reduce the model of a nonlinear dynamic fuel cell stack, which is suitable for control and fault detection studies, is presented. In order to model the fuel cell stack, we have assumed that the fuel cells are arranged in a stack, electrically in series, with thermal and electrical contacts. Since in practical applications a stack may be composed of several (at least fifty) fuel cells, such model will be a large set of differential equations which may be difficult to simulate especially in control applications. In this paper, first, a model for an isolated fuel cell will be given. Then, a model for the temperature distribution in a fuel cell stack will be pursued. Finally, the use of an orthogonal collocation method to reduce the size of the model of the fuel cell stack without changing the model transient or steady state characteristics will be presented.

I. INTRODUCTION

Proton exchange membrane (PEM) fuel cells are the main type of fuel cell developed for ground vehicle applications. Such applications require a fuel cell control, fault detection, and diagnosis. The three major control subsystem loops in a fuel cell system are applied to the air/fuel supply regulation, the water management, and the heat management [1]. In this paper we concentrate on the modeling and simulation of the thermal effects and the temperature distribution in a fuel cell stack.

Existing stack thermal models as in [6] consider the stack as a lumped mass and do not describe thermal distributions in the stack. Typically, these models use a single average cell temperature or stack coolant outlet temperature, as an indicator of the stack thermal condition. However, in a stack, each cell have its own electrical and thermal

*Electronic address: masoud.najafi@inria.fr; INRIA-Rocquencourt

†Electronic address: damiano.di-penta@renault.com; Renault Advanced Electronic Department

‡Electronic address: karim.ben-cherif@renault.com; Renault Advanced Electronic Department

§Electronic address: michel.sorine@inria.fr; SOSSO2 Project, INRIA-Rocquencourt

¶URL: http://www.inria.fr

characteristics different from its neighbors. Furthermore, existing models do not explicitly account for the effect of the end-cells of the stack. The thermal mass of the end-cells draws heat from the cells at both ends of the stack and affects the stack temperature distribution. And above all, the model obtained for the stack is often a large stiff differential equation that is difficult or is not appropriate for real-time applications such as fault detection and process control.

One of the main difficulties in the fuel cell control system is the need for an on-board control and fault detection device to supervise the operation of the system through reliable strategies. These strategies are based on real-time analysis of on-board sensor signals by checking their coherence with mathematical models. The model of each cell includes electrochemical, electrical, and thermal phenomena. Consequently, the large range of transients involved makes the model stiff. The stack model is, then, a large stiff DAE that is too slow for real-time applications. In this paper, we develop a model for fuel cell stack, then we apply the orthogonal collocation method to reduce the model and simulate it with only a few cells. Using the reduced model of stack will be well suited for controllers and diagnosis algorithms.

The one-dimensional, fuel cell stack thermal model developed in this paper considers the features which form an analysis tool for thermal characteristic and fault detection of a PEM fuel cell stack. The fuel cell stack model has been developed with the Modelica language [2]. The Modelica models are then simulated in the Scilab/Scicos (*www.scilab.org*) environment. The developed models of the fuel cell stack consists of N (50, 100) cell, electrically in series, fed with hydrogen-rich reformate and compressed air.

II. FUEL CELL MODEL

In this section, the model of a PEM fuel cell stack is described. Fig. 1 illustrates the global fuel cell system considered in this paper. The reformer processes ethanol, natural gas or gasoline into hydrogen-rich reformate which feeds the

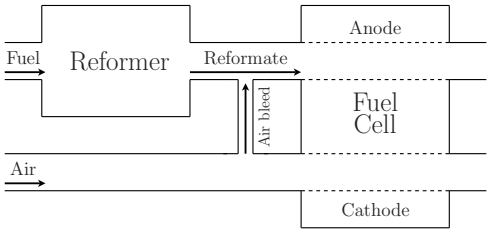

FIG. 1: Fuel cell System

anode of the PEMFC stack whereas the cathode is fed by compressed air. The reformer breaks down hydrocarbons or hydrogen rich fuels into hydrogen, carbon dioxide, carbon monoxide and water. One of the main problems of reforming hydrocarbons is the production of carbon monoxide which is a poison for the stack but this effect can be mitigated

by introducing an air bleed into the anode (see Fig. 1). The model which includes electro-chemical, electrical and thermal phenomena is used to build a model for the fuel cell stack. The internal structure of the fuel cell will not be explained here, interested users are referred to [4–6].

Electrodes of each cell in the stack are supplied by a mass fluid flow q_k^{in} at the temperature T_k^{in}, the pressure P_k^{in} and the mass composition $Y_{i,a}^{in}$, where $i \in \{h, co, n, v, air\}$, and $Y_{i,c}^{in}$, where $i \in \{o, n, v\}$. We suppose that there is no liquid water entering the cell electrodes. The electrochemical reaction produces a current noted I and voltage V_{cell}. The solid temperature is noted T_s and lastly the cell is cooled by a coolant flow q_{cool}^{in} at the temperature T_{cool}^{in}. We define The input variable vector U_k^{in} and output variables vector U_k^{out} of the fuel cell channel $k \in \{a, c, cool\}$ are illustrated in Fig. 2, with

$$
\begin{aligned}
U_a^{in} &= \begin{bmatrix} T_a^{in} & q_a^{in} & P_a^{in} & \lambda_a^{in} & Y_h^{in} & Y_{co}^{in} & Y_{air}^{in} & Y_{va}^{in} \end{bmatrix} \\
U_a^{out} &= \begin{bmatrix} T_a^{out} & P_a^{out} & Y_h^{out} & Y_{wa}^{out} \end{bmatrix} \\
U_c^{in} &= \begin{bmatrix} T_c^{in} & q_c^{in} & P_c^{in} & Y_o^{in} & Y_{vc}^{in} & \lambda_c^{in} \end{bmatrix} \\
U_c^{out} &= \begin{bmatrix} T_c^{out} & P_c^{out} & Y_o^{out} & Y_{wc}^{out} \end{bmatrix} \\
U_{cool}^{in} &= \begin{bmatrix} q_{cool}^{in} & T_{cool}^{in} \end{bmatrix} \\
U_{cool}^{out} &= T_{cool}^{out}
\end{aligned}
$$

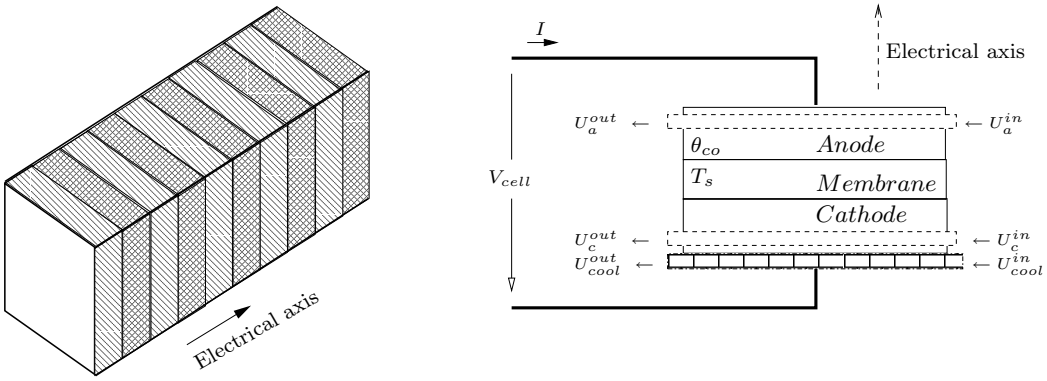

FIG. 2: Fuel cell stack and input and output variables in the fuel cell model

1. Mass balance equations

Mass balance equations are obtained from mass conservation laws. We apply the mass conservation law on hydrogen, oxygen and water in electrodes. Since the procedure to get these equations are identical, we perform it on hydrogen

species, the others are found in a similar way. Let m_h be the hydrogen mass in the anode. Thus, we have

$$\begin{aligned}\frac{dm_h}{dt} &= q_h^{in} - q_h^{out} - M_h\frac{I}{2F} \\ &= q_a^{in}Y_h^{in} - q_a^{out}Y_h^{out} - M_h\frac{I}{2F}\end{aligned}$$

where $\frac{M_h I}{2F}$ indicates the conversion of H_2 to H^+ ions and is obtained from the Faraday law. We suppose that the hydrogen mass in anode m_h is equal to $Y_h^{out}\rho_a V_a$. Assuming a dilute concentration, *i.e.*, $q_a^{out} \approx q_a^{in}$ and ρ_a slightly constant, we get the differential equation (1) for the conservation of hydrogen mass in the anode. In a similar way, the oxygen mass balance equation, *i.e.*, (2), the water mass balance equations in electrodes, *i.e.*, (3) are obtained.

$$\frac{dY_h^{out}}{dt} = \frac{q_a^{in}}{\rho_a V_a}(Y_h^{in} - Y_h^{out}) - \frac{M_h I}{2\rho_a F V_a} \quad (1)$$

$$\frac{dY_o^{out}}{dt} = \frac{q_c^{in}}{\rho_c V_c}(Y_o^{in} - Y_o^{out}) - \frac{M_o I}{4\rho_c F V_c} \quad (2)$$

$$\frac{dY_{w,k}^{out}}{dt} = \frac{q_k^{in}}{\rho_k V_k}(Y_{v,k}^{in} - Y_{w,k}^{out}) + \alpha_k\frac{M_w I}{2\rho_k F V_k} \quad (3)$$

The value of the input mass flows q_k^{in} $k \in \{a, c\}$, are determined as a function of the current I, of the inlet mass fraction of hydrogen and oxygen, noted Y_h^{in} and Y_o^{in}, and of the stoichiometries in the electrodes, noted λ_a and λ_c, as given in (4) and (5).

$$q_a^{in} = \lambda_a\frac{M_h I}{2F Y_h^{in}} \quad (4)$$

$$q_c^{in} = \lambda_c\frac{M_o I}{4F Y_o^{in}} \quad (5)$$

where M_h and M_o are the molar mass of the H_2 and O_2 respectively.

As we will see in the next section, the cell voltage is a function of the amount of reactants inside the electrodes. Thus we define the mean partial pressures of H_2 at the anode and of O_2 at the cathode by

$$\overline{P_h} = \frac{M_a}{2M_h}(Y_h^{in}P_a^{in} + Y_h^{out}P_a^{out}) \quad (6)$$

$$\overline{P_o} = \frac{M_c}{2M_o}(Y_o^{in}P_c^{in} + Y_o^{out}P_c^{out}) \quad (7)$$

where the average molar mass in the cathode and the anode, neglecting the mass fraction of CO and air bleed, will be:

$$M_a = \left(\frac{Y_h^{in}}{M_h} + \frac{Y_{v,c}^{in}}{M_w} + \frac{Y_{n,a}^{in}}{M_{n,a}}\right)^{-1}$$

$$M_c = \left(\frac{Y_o^{in}}{M_o} + \frac{Y_{v,c}^{in}}{M_w} + \frac{Y_{n,c}^{in}}{M_{n,c}}\right)^{-1}$$

where the inlet mass fractions of neutral gas are given by:

$$Y_{n,a}^{in} = 1 - Y_h^{in} - Y_{w,a}^{in} \tag{8}$$

$$Y_{n,c}^{in} = 1 - Y_o^{in} - Y_{w,c}^{in} \tag{9}$$

where the inlet pressures are obtained through a simple pressure drop laws:

$$P_k^{in} = P_k^{out} + K_{dp,k} \frac{q_k^{in}}{P_k^{out}}$$

Finally, we suppose that all the CO and the air bleed is consumed in the the anode:

$$\overline{P_{co}} = \frac{M_a}{2M_{co}} Y_{co}^{in} P_a^{in} \tag{10}$$

$$\overline{P_{air}} = \frac{M_a}{2M_{air}} Y_{air}^{in} P_a^{in} \tag{11}$$

2. Fuel cell voltage

The electrical voltage of a cell can by modeled by the difference between the two electrode potentials and overpotentials, *i.e.*,

$$V_{cell} = E_r - \eta_a - \eta_c - \eta_{ohm} \tag{12}$$

We assume that water is produced in liquid phase, so E_r, the reversible potential, corresponding to the liquid water formation is:

$$E_r = \frac{1}{2F}\left(\Delta H_l^0 - \Delta S_l^0 T_s\right) = E^0 - \frac{\Delta S_l^0}{2F} T_s + \frac{RT_s}{2F} \ln\left(\sqrt{\overline{P_o}}\ \overline{P_h}\right)$$

where E_0, ΔH_l^0, and ΔS_l^0 are the thermo-neutral potential, the variations in standard enthalpy, and standard entropy of liquid water formation, respectively.

The ohmic loss is the voltage loss due to the internal resistance R_{ohm} of the stack cells. Supposing that the membranes are optimally hydrated, we can consider that these resistances are constant, thus the ohmic losses can be computed as given:

$$\eta_{ohm} = R_{ohm} J \tag{13}$$

where J is the current density defined by $I = JA_{act}$ where A_{act} is the active area of a cell.

The anode overpotential η_a is mostly linked to CO poisoning is expression was obtain by Di Penta et al. [7] :

$$\eta_a = \frac{2RT_s}{F} \sinh^{-1}\left(\frac{J}{2(k_{eh}\theta_h + k_{ec}\theta_{co} + k_{res})}\right) \tag{14}$$

where T_s, R, and F are the cell solid temperature, the gas constant, and the Faraday constant. σ is the density of sites on the catalyst layer. The coverage fractions of carbon monoxide and hydrogen carbon monoxide on the anode catalyst sites noted θ_{co} and θ_h are given by

$$\sigma\frac{d\theta_{co}}{dt} = \left(k_{fc}\overline{P_{co}} - \frac{k_{fo}k_{oc}\theta_{co}\overline{P_{air}}}{k_{oc}\theta_{co}+k_{oh}\theta_h+b_{fo}k_{fo}}\right)(1-\theta_h-\theta_{co}) - b_{fc}k_{fc}\theta_{co} - \frac{k_{ec}\theta_{co}J}{k_{eh}\theta_h+k_{ec}\theta_{co}+k_{res}} \quad (15)$$

$$\theta_h = \frac{k_{fh}\overline{P_h}}{k_{fh}\overline{P_h}+b_{fh}k_{fh}}(1-\theta_{co}) - \frac{J}{k_{fh}\overline{P_h}+b_{fh}k_{fh}} \quad (16)$$

with

$$b_{fc} = b_{fc}^0 \exp\left(\frac{-E_{bfc}}{RT_s}\right)$$

where $\overline{P_{co}}$, $\overline{P_{air}}$, $\overline{P_h}$, are the mean partial pressures of CO, air bleed, and H_2 at the anode which were defined (6), (10) and (11).

Contrary to the anode, the cathode is not a place of competing reactions. Nevertheless, the cathode is at the origin of most of the activation and diffusion losses. The cathode overpotential is given by:

$$\eta_c = \frac{2RT_s}{F}\sinh^{-1}\left(\frac{k_{diff}\overline{P_o}J}{2k_{act}(k_{diff}\overline{P_o}-J)}\right) \quad (17)$$

where

$$k_{act} = k_{act}^0 \exp\left(\frac{-E_{kact}}{RT_s}\right),\ k_{diff} = k_{diff}^0 \exp\left(\frac{-E_{kdiff}}{RT_s}\right)$$

where $\overline{P_o}$ is defined in (7).

3. Fuel cell thermal model

We suppose that solid part of the fuel cell is isothermal and the temperature of fluids at the outlet of the cell is the same as the temperature of the fluids inside the cell. We have also supposed that the specific heat capacity of elements are constant. We have considered four thermal equations in each cell, *i.e.*, an equation for the solid mass equation, two equations for anode and cathode gases, and an equation for the coolant. The fuel cell solid temperature T_s is obtained with the first law of thermodynamics, *i.e.*,

$$m_s C_{p,s}\frac{dT_s}{dt} = W_{trans} + W_{prod} \quad (18)$$

where m_s and $C_{p,s}$ are the mass and the specific heat capacity of the solid, respectively. W_{trans} which is the heat transfer to the solid is obtained as the total thermal energy transfered from existing species in the electrodes to the solid. Using the Newton law of cooling, we get

$$W_{trans} = h_a S_a\left(T_a^{out}-T_s\right) + h_c S_c\left(T_c^{out}-T_s\right) + h_{cool}S_{cool}(T_{cool}^{out}-T_s) \quad (19)$$

where $h_a S_a$, $h_c S_c$, and $h_{cool} S_{cool}$ are the heat transfer coefficients between the solid and the gas in the anode, the gas in the cathode, and the coolant, respectively. As shown in Fig. 3, it is assumed that the chemical power of hydrogen is shared between electrical power and the heat generation from reactions. Supposing that reactions take place on

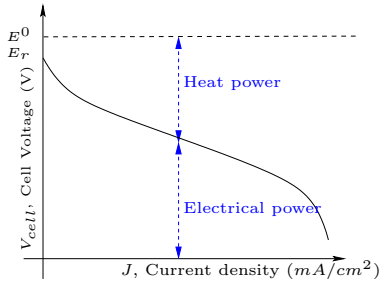

FIG. 3: Thermal balance in the fuel cell

the catalyst (solid), we obtain the heat generation as a function of the current density J and the cell voltage V_{cell}, as given in 20.

$$W_{prod} = (E^0 - V_{cell})I \tag{20}$$

Differential equations describing thermal behavior of fluids in electrodes are

$$V_k \rho_k C_{p,k} \frac{dT_k^{out}}{dt} = W_{k,evap/cond} + W_{k,trans}, \quad k \in \{a, c\} \tag{21}$$

where $W_{k,evap/cond}$ is the heat transfered from evaporation/condensation which is obtained from

$$W_{k,evap/cond} = q_k L_v (Y_{wk}^{in} - Y_{vk}^{out}), \quad k \in \{a, c\} \tag{22}$$

where L_v is the latent heat of water. $W_{k,evap/cond}$ is the heat transfered from the solid to gas is obtained from

$$W_{k,trans} = q_k^{in} C_{p,k} (T_k^{in} - T_k^{out}) + h_k S_k \left(T_s - T_k^{out}\right), \quad k \in \{a, c\} \tag{23}$$

Finally, the thermal behavior of the coolant the is given by:

$$m_{cool} C_{p,cool} \frac{dT_{cool}^{out}}{dt} = q_{cool}^{in} C_{p,cool} \left(T_{cool}^{in} - T_{cool}^{out}\right) + h_{cool} S_{cool} \left(T_s - T_{cool}^{out}\right) \tag{24}$$

4. Fuel cell complete model

The complete model of the fuel cell is an ODE with eight state variables. Defining state and input vectors as

$$X = [Y_h^{out}, Y_o^{out}, Y_{w,a}^{out}, Y_{w,c}^{out}, \theta_{co}, T_a^{out}, T_c^{out}, T_{cool}^{out}]^T$$

$$U = [I, Y_h^{in}, Y_{co}^{in}, Y_{air}^{in}, Y_o^{in}, Y_{w,a}^{in}, Y_{w,c}^{in}, q_a^{in}, q_c^{in}, q_{cool}^{in}, P_a^{out}, P_c^{out}, T_a^{in}, T_c^{in}, T_{cool}^{in}]^T,$$

Inputs	Values	Inputs	Values	Inputs	Values	Inputs	Values
Y_h^{in}	0.025	Y_o^{in}	0.2	Y_{co}^{in}	4.5E-5	Y_{air}^{in}	0.018
$Y_{w,a}^{in}$	0.33	$Y_{w,c}^{in}$	0.13	T_a^{in}	350 K	T_c^{in}	337 K
P_a^{out}	1.5 Atm	P_c^{out}	1.5 Atm	λ_a	1.38	λ_c	1.81
q_{cool}^{in}	7.3 gr/sec	T_{cool}^{in}	346 K	I	150 A		

TABLE I: Input variable values

we can summarize the model as follows

$$
\begin{aligned}
m_s C_{p,s} \frac{dT_s}{dt} &= h_a S_a \left(T_a^{out} - T_s\right) + h_c S_c \left(T_c^{out} - T_s\right) + h_{cool} S_{cool} \left(T_{cool}^{out} - T_s\right) + (E^0 - V_{cell}) I \\
\frac{dX}{dt} &= A(X, T_s, U) \\
V_{cell} &= G(X, T_s, U)
\end{aligned}
$$

This model has been implemented and the experimental data are used to identify and validate the model parameters, see [6]. We have used the Modelica language [2, 8] to model the fuel cell. The Modelica model is then simulated in Scicos [3]. In this simulation, we have used the input variables which are given in table **I**. In Fig. 4 the polarization curve of the fuel cell which we obtained is plotted.

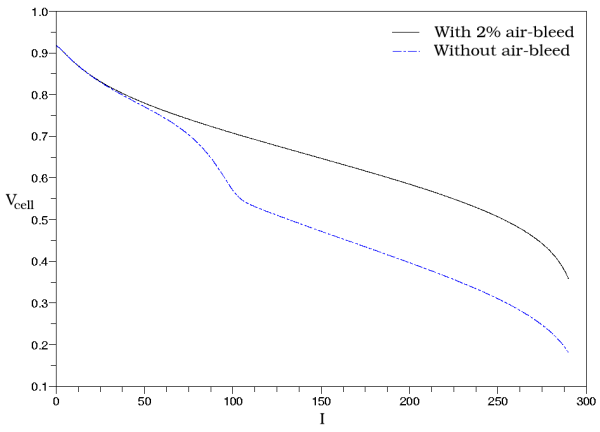

FIG. 4: Polarization curve of the fuel cell, with and without air bleed

III. A THERMAL MODEL FOR THE FUEL CELL STACK

Most papers published in the fuel cell modeling domain assume that all cells in a fuel cell stack are identical, consequently modeling and simulation of a stack is reduced to the modeling and simulation of a single fuel cell. Although, this assumption is reasonable for many cases, there are situations where this assumption does not hold;

e.g., a stack with some faulty cells, or a fuel cell stack whose cells have different thermal or chemical characteristics. Based on an evaluation of existing stack thermal models in the literature, we build a thermal model for the stack.

We assume a fuel cell stack composed of cells electrically in series with thermal and electrical contacts. The stack model is a 1-D model in which fuel cells are independent and each cell can only influence the others via thermal conduction. Although a cell is composed of several layers, we assume that the cells are lumped plates of width δ and mass m_s. Each cell is in thermal contact with two adjacent cells and the input of all cells are identical except the coolant electrodes. In fact, here we assume that the cooling circuit does not pass through all cells. Generally, five or even more cells are cooled down by a single cooling plate. In Fig. 5 the cooling channel layout of our fuel cell stack is given. Thus, Q^{in}_{cool}, the flow rate of the coolant in the stack channels is defined as

$$q^{in}_{cool}(i) = \begin{cases} q^{in}_{cool,0} & \texttt{if} \quad i = 5, 10, 15, ... \\ 0 & \texttt{else} \end{cases}$$

where $q^{in}_{cool,0}$ is the coolant flow in a 'cooled' cell, see Fig. 5.

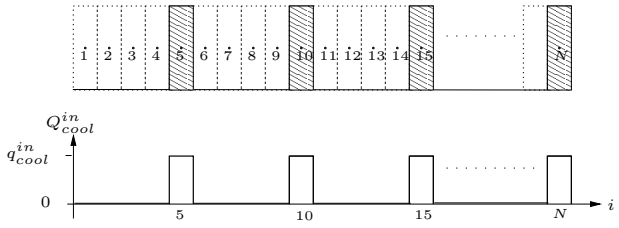

FIG. 5: Q^{in}_{cool} in the fuel cell stack

In the stack, each cell affects the two adjacent cells through thermal conduction. Thus, the model of i^{th} cell in the stack is

$$\begin{cases} m_{s,i}C_{s,i}\dfrac{dT_{s,i}}{dt} &= h_a S_a \left(T^{out}_{a,i} - T_{s,i}\right) + h_c S_c \left(T^{out}_{c,i} - T_{s,i}\right) + h_{cool} S_{cool}(T^{out}_{cool,i} - T_{s,i}) + (E^0 - G(X_i, T_{s,i}, U_i))I + \psi_i \\ \dfrac{dX_i}{dt} &= A(X_i, T_{s,i}, U_i) \\ V_{cell,i} &= G(X_i, T_{s,i}, U_i) \end{cases} \tag{25}$$

where ψ_i is defined as

$$\psi_i = \begin{cases} \frac{D}{\delta}\left(T_{s,2} - T_{s,1}\right) + h_{inf} S_{inf}(T_{inf} - T_{s,1}) & i = 1 \\ \frac{D}{\delta}\left(T_{s,N-1} - T_{s,N}\right) + h_{inf} S_{inf}(T_{inf} - T_{s,N}) & i = N \\ \frac{D}{\delta}\left(T_{s,i-1} + T_{s,i+1} - 2T_{s,i}\right) & 1 < i < N \end{cases} \tag{26}$$

The terminal voltage of the stack is

$$V_{stack} = \sum_{i=1}^{N} V_{cell,i} = \sum_{i=1}^{N} G(X_i, T_{s,i}, U_i)$$

The simulation result of a stack composed of 100 cells is given in Fig. 6. For this simulation we have used the parameters given in the table **I**. In Fig. 6, the temperatures of the first twenty cells of the fuel cell stack (*i.e.*, $T_{s,i}, \quad i = 1, \cdots, 20$) are given for the time interval, time=$[0, 70]$ seconds. Fig. 7 gives the value of $T_{s,i}, \quad i = 1, \cdots, 20$ at time=70 sec. In this simulation, the initial cell temperatures are $300K$.

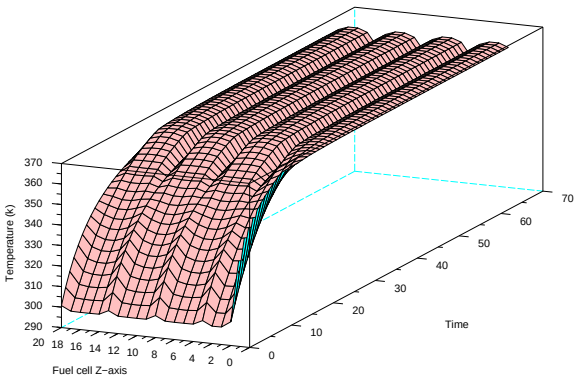

FIG. 6: Temperature distribution in the stack of 100 fuel cells

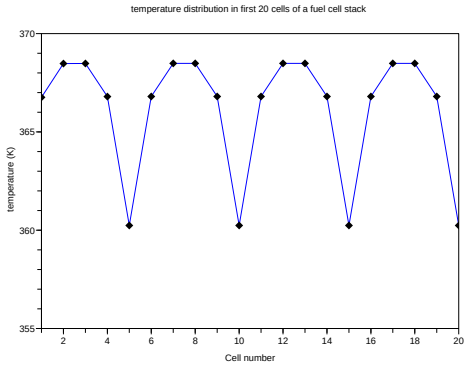

FIG. 7: Temperature distribution in the stack at t=70 sec

A typical fuel cell stack is composed of at least 50 fuel cells. Modeling such a stack usually ends up with a large stiff differential equation. Consequently, the simulation of the model will be slow. In some applications such as fault detection where the output of a physical system is compared with the output of a model, we need a real-time simulation. Thus, a compromise between low model complexity and high solution accuracy should be found. Therefore, a functional approximation method is necessary to obtain a lower model size as well as an accurate enough modeling and simulation.

IV. MODELING OF THE FUEL CELL STACK AS A 1D PDE

The dynamics of a single fuel cell is described by an ODE and the fuel cell stack model (25,26) developed in section III is composed of N cells in series with thermal and electrical contacts. This model is too large and too slow to be used in control applications. In order to come up with a solution for this problem and obtain a reduced model, the stack model is transformed into a partial differential equation (PDE). For that, we assume that the stack is a uniform mass whose thermal behavior is given by the following general PDE and two Robin's type boundary conditions. For the sake of simplicity, in the rest of the paper we assume that cooling channels pass through all cells. Thus, the model of stack (25,26) can be considered as the PDE (27) discretized at N distinct points.

$$\begin{cases} \dfrac{\partial \mathcal{X}}{\partial t} &= A(\mathcal{X}, \mathcal{T}_s, U) \\ c_0 \dfrac{\partial \mathcal{T}_s}{\partial t} &= c_1 \dfrac{\partial^2 \mathcal{T}_s}{\partial z^2} + c_2(\mathcal{T}_a^{out} - \mathcal{T}_s) + c_3(\mathcal{T}_c^{out} - \mathcal{T}_s) + c_4(\mathcal{T}_{cool}^{out} - \mathcal{T}_s) + (E^0 - G(\mathcal{X}, \mathcal{T}_s, U))I \\ 0 &= c_5 \dfrac{\partial \mathcal{T}_s}{\partial z} + c_2(\mathcal{T}_a^{out} - \mathcal{T}_s) + c_3(\mathcal{T}_c^{out} - \mathcal{T}_s) + c_4(\mathcal{T}_{cool}^{out} - \mathcal{T}_s) + c_7(\mathcal{T}_{inf} - \mathcal{T}_s) + (E^0 - G(\mathcal{X}, \mathcal{T}_s, U))I|_{z=0} \\ 0 &= c_6 \dfrac{\partial \mathcal{T}_s}{\partial z} + c_2(\mathcal{T}_a^{out} - \mathcal{T}_s) + c_3(\mathcal{T}_c^{out} - \mathcal{T}_s) + c_4(\mathcal{T}_{cool}^{out} - \mathcal{T}_s) + c_7(\mathcal{T}_{inf} - \mathcal{T}_s) + (E^0 - G(\mathcal{X}, \mathcal{T}_s, U))I|_{z=L} \end{cases} \tag{27}$$

where $\mathcal{T}_s$, and $\mathcal{X}$ are the temperature and state variables of the uniform mass as a function of z and relates to $T_{s,i}$ and X_i via

$$\begin{cases} T_{s,i} &\approx \mathcal{T}_s(z)|_{z=(i-1/2)\delta}, \quad i = 1, \cdots, N \\ X_i &\approx \mathcal{X}(z)|_{z=(i-1/2)\delta}, \quad i = 1, \cdots, N \end{cases}$$

The coefficients c_j, where $i \in 0 \cdots 7$, are unknowns that can be obtained if we discretize the PDE via the finite difference method and compare the resulting ODE with original stack model (25,26). The coefficients can then be computed as given in the following table.

$c_0 = m_s C_s$	$c_1 = D\delta$	$c_2 = h_a S_a$	$c_3 = h_c S_c$
$c_4 = h_{cool0} S_{cool}$	$c_5 = D$	$c_6 = -D$	$c_7 = h_{inf} S_{inf}$

The obtained PDE can be solved instead of simulating the stack. But the simulation of a PDE is not a trivial task and needs a discretization of the space at several points to have a reasonable accuracy. There are, however, some spectral methods to discretize a PDE using only a small number of discretization points which will be explained in the next section.

V. THE COLLOCATION METHOD

The collocation method, which is a useful method for solving PDEs, was developed originally as a stable, predictable, and simple way to implement pseudo-spectral technique. Because of its reliability, it has become a standard method

for solving boundary-value problems by polynomial trial function expansions. This method allows discretizing a PDE with a selection of only 3 to 7 points in the region, comparing to 10 to 20 points in finite difference method [9–11].

The formulation of this method is based on choosing a set of trial functions from an orthogonal polynomial sequence, with the discretization points computed as the roots of the polynomial next in the sequence. Similar to the finite difference method, in collocation methods N_c points are selected which partition the region into $N_c + 1$ segments. Then, $\Phi(z,t)$ is approximated by a Lagrange interpolation polynomial $\hat{\Phi}(z,t)$ of order N_c+1 using z_i as interpolation points. Then, the approximated partial derivatives at z_i (corresponding derivatives of $\hat{\Phi}(z,t)$) are inserted in the PDE to satisfy the PDE only at collocation points z_i. To implement this method in a 1-D region with N_c collocation points, Φ and its partial derivatives are approximated as linear combinations of basis functions L_i, *i.e.*,

$$\Phi(z,t) \approx \hat{\Phi}(z,t) = \sum_{i=1}^{N_c} \hat{\Phi}_i(t) L_i(z) \tag{28a}$$

$$\Rightarrow \frac{\partial \Phi(z,t)}{\partial z} \approx \frac{\partial \hat{\Phi}(z,t)}{\partial z} = \sum_{i=1}^{N_c} \hat{\Phi}_i(t) \frac{dL_i(z)}{dz} \tag{28b}$$

$$\Rightarrow \frac{\partial^2 \Phi(z,t)}{\partial z^2} \approx \frac{\partial^2 \hat{\Phi}(z,t)}{\partial z^2} = \sum_{i=1}^{N_c} \hat{\Phi}_i(t) \frac{d^2 L_i(z)}{dz^2} \tag{28c}$$

$$\Rightarrow \frac{\partial \Phi(z,t)}{\partial t} \approx \frac{\partial \hat{\Phi}(z,t)}{\partial t} = \sum_{i=1}^{N_c} \frac{d\hat{\Phi}_i(t)}{dt} L_i(z) \tag{28d}$$

$L_i(z)$ are the N_c+1 linearly independent basis functions of the N_c^{th} order Lagrange polynomial. They are determined by the $N_c + 1$ collocation points z_i as follows:

$$L_i(z) = \prod_{j=1,\ i\neq j}^{N_c} \frac{z - z_j}{z_i - z_j} = \sum_{k=1}^{N_c} a_k z^k \tag{29}$$

The coefficients a_k can be computed from the known points z_i. Hence, the derivatives of the Lagrange-Polynomial (29) can be obtained easily as given in (30).

$$\frac{dL_i(z)}{dz} = \sum_{k=1}^{N_c} k a_k z^{k-1} \tag{30a}$$

$$\frac{d^2 L_i(z)}{dz^2} = \sum_{k=2}^{N_c} k(k-1) a_k z^{k-2} \tag{30b}$$

Since the PDE is to be satisfied only at the collocation points and the Lagrange polynomials (29) have the property (31). Thus the derivatives of the Lagrange polynomials (31) at the collocation points are obtained to be used to compute (28).

$$\begin{cases} L_i(z_j) = 1 & \texttt{for}\ \ i = j \\ L_i(z_j) = 0 & \texttt{for}\ \ i \neq j \end{cases} \tag{31}$$

The interpolation with the Lagrange polynomials tends to provide oscillating curves yielding a very bad approximation, if the collocation points (z_i) are not well chosen. In order to avoid this problem, the basis functions of the Lagrange polynomial should be a set of orthogonal functions in the interval $0 \leq \xi \leq 1$ with respect to some weighting

function $w(\xi)$ assuming a normalized ξ-domain with $L = 1$. When the interpolation points ξ_i are chosen as roots of Jacobi polynomials, the Lagrange polynomials are orthogonal in the sense of

$$\int_0^1 w(\xi)L_i(\xi)L_j(\xi)d\xi \texttt{ for } i \neq j, \quad w(\xi) = (1-\xi)^{\tau_1}\xi^{\tau_2} \tag{32}$$

The Jacobi polynomial of order N is defined as:

$$P_N^{(\tau_1,\tau_2)} = \sum_{i=0}^{N}(-1)^{N-i}\zeta(N,i)\xi^i$$

The function $\zeta(N,i)$ can be computed recursively as follows:

$$\zeta(N,i) = \tfrac{N-i+1}{i}\,\tfrac{N+i+\tau_1+\tau_2}{i+\tau_2}\zeta(N,i-1)$$
$$\zeta(N,0) = 1$$

where the parameters τ_1 and τ_2 can be used to influence the position of collocation points (ξ_i). This results from the weighting function $w(\xi) = (1-\xi)^{\tau_1}\xi^{\tau_2}$. If τ_1 is small, the concentration of collocation points will be toward $\xi = 1$ and when τ_2 is small, the concentration of collocation points will be around $\xi = 0$. The concentration will be uniform in the region, if $\tau_1 = \tau_2$.

VI. APPLICATION

As a simple application, the orthogonal collocation method is used to discretize the PDE (27) using six collocation points. The simulation result is given in Fig. 8. In this figure, the temperature of the stack is given as a function of time and z. In order to compare the simulation result, the original fuel cell, composed of 50 cells, was simulated

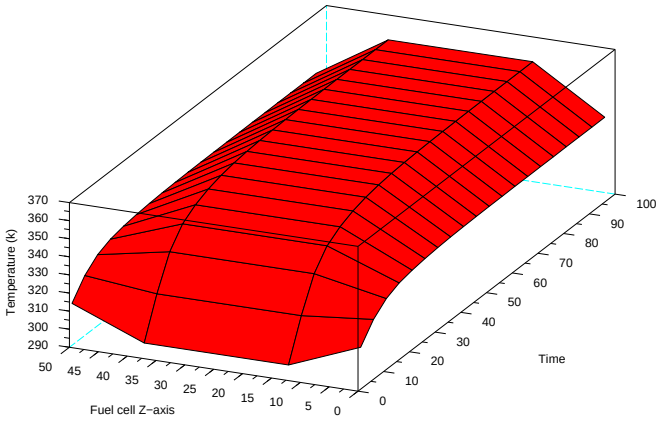

FIG. 8: Simulation of a fuel cell stack with the orthogonal collocation method using four discretization points

with the same parameters and input vector (U). The result of two simulations is given in Fig. 9. In this figure, the

temperature of stack via two method is given. The initial temperature is 293K and the steady state temperature is about 420K. The simulation shows that two results are nearly identical.

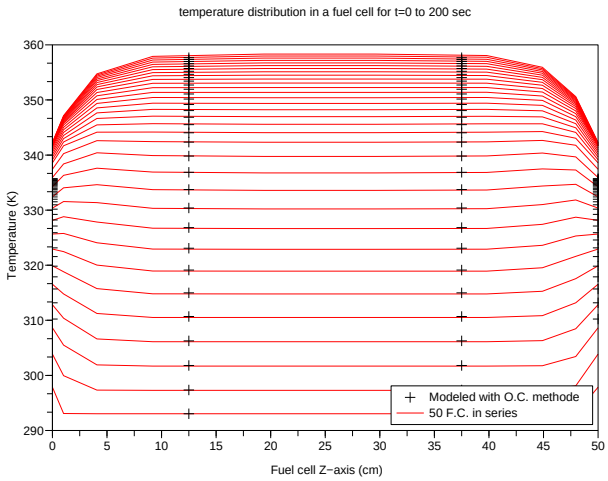

FIG. 9: Temperature distribution (in time and z) in a fuel cell stack using two simulation methods

In order to demonstrate the efficiency of the collocation method in simulation of cell cell stacks, we simulate a fault in a fuel cell. Consider a fuel cell stack composed of 50 cells, and suppose that due to a fault, cooling circuit in cell numbered 24, 25, 26, and 27 is blocked and these cells are not cooled down properly. We have modeled such a fault by replacing coolant flow rate ($q^{in}_{cool}(i)$) in the faulty cells in the stack in (24,25,26) by equation (33).

$$q^{in}_{cool}(i) = \begin{cases} 0.5q^{in}_{cool,0} & \texttt{for } i = 24, 25, 26, 27 \\ q^{in}_{cool,0} & \texttt{other } i \end{cases} \tag{33}$$

Similar to the previous example, two methods are used; A model composed of 50 cells with a fault, and another model with orthogonal collocation method. In the collocation method, we assume that the stack is composed of three regions and we discretize each region with four points ($N_c = 4$). So, the total number of collocation points is twelve. The τ_1 and τ_2 of each domain are chosen so that the concentration of the points around the faulty region become higher. In Fig. 10 and 11, the temperature of the cell is given as a function of z and time. The simulation shows a very good accordance between the simulation of the stack of 50 cells and the simulation of the stack simulated with only 12 cells.

VII. CONCLUSION

The reaction-diffusion model of fuel cell stack which may be composed of at least 50 cells is modeled and simulated with a small number of cells. We have used the orthogonal collocation method to sample the stack at only a few points, which is quite lower than the number of cells in the stack. The main principle of the orthogonal collocation

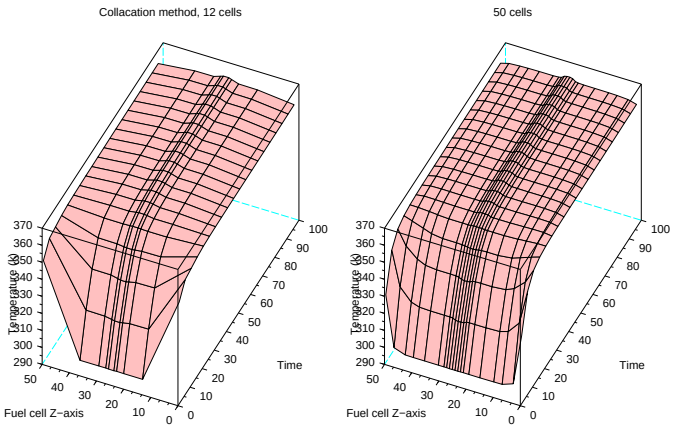

FIG. 10: Simulation result of a faulty fuel cell stack with multi-domain collocation method and standard method of the stack of 50 cells

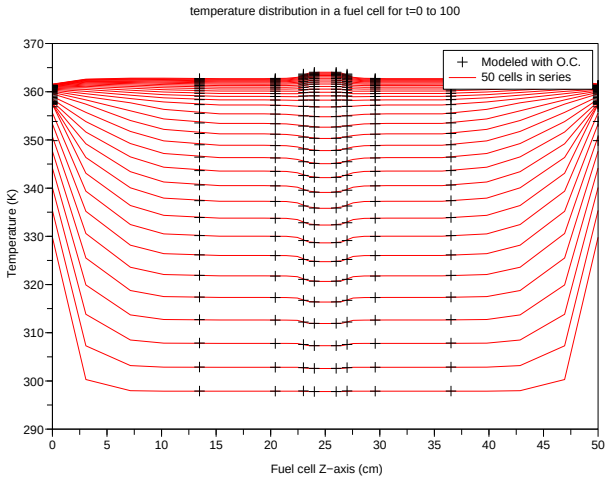

FIG. 11: 2D simulation of a faulty fuel cell stack at differed simulation times

method is that the material and energy balances remains unchanged and they are still satisfied exactly at collocation points. Therefore the model of stack via the collocation method becomes smaller and easier to simulate. There are several advantages when using the reduced model: the model of the fuel cell stack is no longer discrete, which allows a uniform modeling. Then, this method reduces the size of the process model in terms of number of variables and balances leading to significant computational savings.

Nomenclature

A_{act}= the active membrane area

b_i= kinetics constants $i \in \{fh, fc, fo\}$

C_e= specific heat capacity of elements $e \in \{\ s,\ a,\ c,\ cool\ \}$

D= heat transfer coefficients between two adjacent cells

E_i= activation energies $i \in \{bfc, kact, kdiff\}$

E^0= thermo-neutral potential (1.48 volts)

F= Faraday constant (96450 $coulombs/mol$)

$h_k S_k$= heat transfer coefficients between electrodes and gas $k \in \{a, c\}$

$h_{cool} S_{cool}$= heat transfer coefficient between solid and coolant

$h_{inf} S_{inf}$= heat transfer coefficient between end-cells and the environment

I, J= current of the cell and the current density ($I = JA_{act}$)

k_i= kinetics constants $i \in \{fh, eh, fc, ec, fo, oh, oc, res\}$

k_i^0= kinetics constants $i \in \{act, diff\}$

L= the fuel cell stack length

M_f= molar mass of fluids $f \in \{\ h,\ o,\ co,\ w,\ air\ \}$

$M_{n,k}$ = average molar mass of neutral gases in electrodes $k \in \{a, c\}$

P_k^{out}= output pressure in electrodes $k \in \{a, c\}$

q_{cool}^{in}= inlet coolant mass flow

R= gas constant (8.314 $J/(mol\ K)$)

R_{ohm}= ohmic resistance of a cell

T_k^{in}= inlet fluid temperature at the electrodes $k \in \{a, c\}$

T_{cool}^{in}= inlet coolant temperature

T_s= solid temperature

T_k^{out} = outlet fluid temperature at the electrodes $k \in \{a, c\}$

T_{cool}^{out}= outlet coolant temperature

T_{inf}= environment temperature

V_{cell}= cell voltage

V_k= volume of electrode channels $k \in \{a, c\}$

Y_h^{in}= anode inlet mass fraction of H_2

Y_{co}^{in}= anode inlet mass fraction of CO

Y_{air}^{in}= anode inlet mass fraction of air bleed

Y_o^{in}= cathode inlet molar fraction of O_2

$Y_{v,k}^{in}$= inlet mass fraction of vapor water at electrodes $k \in \{a, c\}$

Y_h^{out}= anode outlet mass fraction of H_2

Y_o^{out} = anode outlet mass fraction of O_2 in cathode

$Y_{w,k}^{out}$= outlet mass fraction of water at the electrodes $k \in \{a, c\}$

Greek

ΔS_l^0= change in entropy of liquid water formation under the standard condition

ΔH_l^0= change in enthalpy of liquid water formation under the standard condition

δ= The thickness of a single fuel cell

ρ_k= average mass density of gas in electrodes $k \in \{a, c\}$

λ_k= inlet stoichiometric ratio at the electrodes $k \in \{a, c\}$

α_k = water transfer coefficient through membrane in electrodes $k \in \{a, c\}$ and $\alpha_a = 1 - \alpha_c$

θ_{co}= anode catalyst CO poisoning rate

β_k= pressure drop parameter in electrodes $k \in \{a, c\}$

Subscripts

a=Anode

c= Cathode

o=O_2

h=H_2

co=CO

n= neutral gas

air= air bleed

w= water

v= vapor water

l= liquid water

s= solid mass

$cool$=coolant

Superscripts

in= Input to the cell

out= Output from the cell

---

[1] J. Pukrushpan, A. Stefanopoulou and H. Peng. Modeling and control for PEM fuel cell stack system. *IEEE American Control Conference*, 2002.

[2] P. Fritzson. Principles of Object-Oriented Modeling and Simulation with Modelica 2.1. *Wiley-IEEE Press*, 2002.

[3] S. L. Campbell and J-Ph. Chancelier and R. Nikoukhah, Modeling and simulation Scilab/Scicos, *Springer Verlag*, 2005.

[4] Jung S. Yi and Trung V. Nguyen. An Along-the-Channel Model for Proton Exchange Membrane Fuel Cells. *Journal of*

Electrochemical Society, 1149–1159, 1998.

[5] M. M. Mench and C.Y. Wang and S. Thynell. An Introduction to Fuel Cells and Related Transport Phenomena, *Journal of Transport Phenomena*, vol. 145, 2001.

[6] D. DiPenta and K. Bencherif and M. Sorine and Q. Zhang. A Reduced Fuel Cell Stack Model for Control and Fault Diagnosis. *Journal of Fuel Cell Technology*, Volume 3, Issue 4, pp. 384-388, 2006.

[7] D. DiPenta and K. Bencherif and Q. Zhang and M. Sorine. Fuel Cell Carbon Monoxide Poisoning Estimation and Control with Air Bleed Injection. *IEEE Conference on Control Application, Munich, Germany*, 2006.

[8] M. Najafi and R. Nikoukhah and S. Steer and S. Furic. New features and new challenges in modeling and simulation in Scicos. *IEEE Conference on Control Application, Toronto, Canada*, 2005.

[9] J. Villadsen and M. Michelsen. Solution of Differential Equation Models by Polynominal Approximation. *Prentice-Hall*, 1982.

[10] R. G. Rice and D. D. Do. Applied Mathematics and Modeling for Chemical Engineers. *Wiley*, 1995.

[11] Manuel Pereira Remelhe and Jochen Till. Modeling of Dynamic Systems, 2005.